Nanoscale

Accepted Manuscript

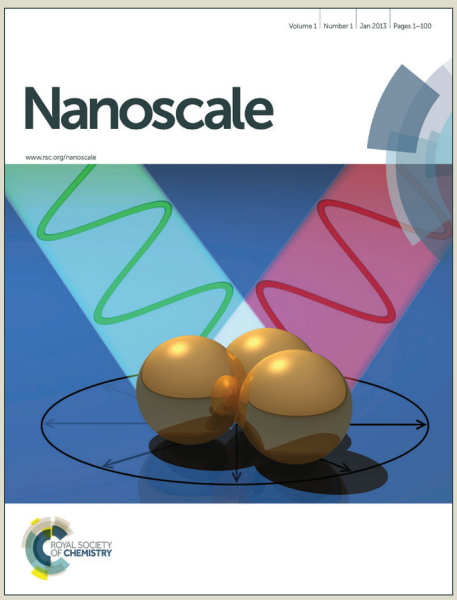

ROYAL SOCIETY OF CHEMISTRY

www.rsc.org/nanoscale

Journal Name

ARTICLE

Probing the Mechanism of Plasma Proteins Adsorption on Au and Ag Nanoparticles with FT-IR Spectroscopy

Received 00th January 20xx,
Accepted 00th January 20xx

DOI: 10.1039/x0xx00000x

www.rsc.org/

Mengmeng Wang[a], Cuiping Fu[a], Xingang Liu[a], Zhipeng Lin[b], Ning Yang[b]* and Shaoning Yu[a]*

Abstract: Protein-nanoparticle interactions are important in the biomedical application of nanoparticles and for growing biosafety concerns about nano materials. In this study, the interactions of four plasma proteins, human serum albumin (HSA), myoglobin (MB), hemoglobin (HB), and trypsin (TRP), with Au and Ag nanoparticles were investigated by FT-IR spectroscopy. The secondary structure of thio-proteins changed with time during incubation with Au and Ag nanoparticles, but the secondary structures of non-thio-proteins remained unchanged. The incubation time for structural changes depended on the sulfur-metal bond energy; the stronger the sulfur-metal energy, the less time needed. H/D exchange experiments revealed that protein-NP complexes with thio-proteins were less dynamic than free proteins. No measurable dynamic differences were found between free non-thio-proteins and the protein-Au (or Ag) nanoparticles complex. Therefore, the impact of covalent bonds on protein structure is greater than that of the electrostatic force.

Introduction

Protein-nanoparticle (NP) interactions are important in the biomedical application of NPs.[1-11] NPs are small enough to enter almost all areas of the body, leading to potentially new approaches in medicine or even biological hazards.[1,2] When entering the body, NPs make contact with biological fluids, such as plasma. In the physiological environment, NPs selectively bind proteins to form a 'protein corona'.[1,2] This is almost always a first step when NPs enter a biological fluid,[1,3,4] and this corona likely determines the fate of the NPs *in vivo*.[12] Formation of the 'protein corona' may lead to an altered conformation and further perturb protein function. Thus, understanding how and why proteins are adsorbed to NPs is of prime importance.[13,14] The mechanism underlying protein adsorption on NPs is a challenging problem, as minor changes in protein structure or conformation can affect protein stability and its functional properties.[1]

Gold nanoparticles (AuNPs) have received increasing attention in all fields of science in the past few decades due to their attractive physicochemical properties,[2,14] and have been investigated vigorously as a promising drug delivery platform, as well as transfection vectors,[15,16] DNA-binding agents,[17,18] protein inhibitors, and spectroscopic markers. All of these features have great potential in biomedical applications.[19,20] Both thiol groups and organic disulfides have been reported to be prone to sulfur-Au coordination on the gold surface and easily suffer some structural changes at the surface of AuNPs.[21,22] However, these studies generally failed to recognize the reaction mechanism between proteins and NPs.

Despite nanoscience has remarkablely developed in recent years, the nature of the interactions between NPs and proteins is not well understood, which being a significant hurdle for the use of NPs in medical and biological applications.[23,24] The forces involved in protein-NPs interactions are mainly Van der Waals forces, electrostatic binding, hydrogen bonds, hydrophobic force, and covalent bonds[25,26] (Scheme 1). One of the most common synthetic methods for preparing AuNPs is based on citrate reduction and stabilization. Citrate anions reduce gold ions to atoms and stabilize colloidal AuNPs.[27] The reason for the stability of AuNPs in aqueous solution is that the COO^- on AuNPs interacts with H_2O to form hydrogen bonds. Proteins and AuNPs can also form hydrogen bonds.[26,28] The hydrogen bonds between protein and AuNP are very complex that we can attribute them to electrostatic forces (ionic interactions and hydrogen bonds).[28] The Van der Waals forces are much weaker than other forces and are usually neglected, though they have a truly pervasive impact.[29] Protein-AuNP interactions do not include hydrophobic force. Therefore, the absorption of protein on AuNPs is due mainly to electrostatic forces[30] and covalent bonds (Au-S coordination). Wang et al found that disulfide bonds in the protein directly recognize the gold surface and form Au−thiol coordination bonds (Au−S). The interaction between proteins and AuNPs includes initial electrostatic adsorption followed by Au−S coordination, which determines the transformation in secondary structures.[3] Previous work in our laboratory also revealed that the structural change in HSA absorbed on AuNPs is related to the sulfur-Au interaction.[21]

a. Department of Chemistry, Fudan University, Shanghai 200433, China.
b. Fifth Department of Hepatic Surgery, Eastern Hepatobiliary Surgery Hospital, Secondary Military Medical University, Shanghai 200438, China.
*Correspondence to: Shaoning Yu, Email: yushaoning@fudan.edu.cn and Ning Yang, Email:lancet829@gmail.com

The goal of the present study was to further address the mechanism of plasma protein absorption on AuNPs. FT-IR secondary derivative spectroscopy was employed to determine the structural changes in absorbed proteins, and the FT-IR H/D exchange method was used to compare the dynamic properties of free and absorbed proteins. In order to probe protein absorption and the structural mechanism, four plasma proteins (two thio-proteins, namely human serum albumin (HSA) and trypsin (TRP), and two non-thio-proteins, namely hemoglobin (HB) and myoglobin (MB) and Au/AgNPs were used in these experiments. The relationship between protein structure changes over time and sulfur-metal bond energies were also addressed by comparing proteins absorbed on AuNPs and AgNPs.

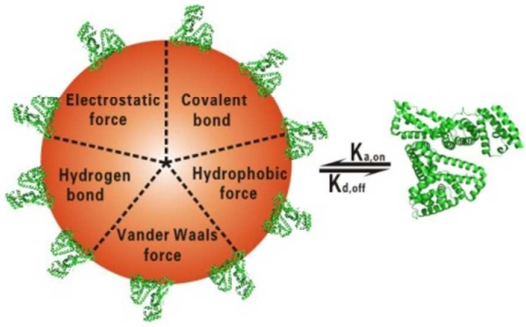

Scheme 1. The forces involved in protein-AuNP interactions. Schematic representation of a protein absorbed on a nanoparticle, illustrating the exchange processes.

Results and Discussion

FT-IR is an excellent tool for the structural characterization of proteins in various environments and is a valuable method for monitoring changes in the secondary structure of proteins.[31,32] The second-derivative spectrum of the amide I band (1700-1600 cm^{-1}) has been widely used to quantify the secondary structural composition of proteins and polypeptides.[14] A major advantage of FT-IR spectroscopy for structural characterization is that it is not limited by protein size or the physical state of the samples. In order to probe the effect of the S-Au interaction on the secondary structures of proteins, four plasma proteins (two thio-proteins: HSA and TRP, and two non-thio-proteins: HB and MB) were employed in these experiments. The FT-IR analysis of these four plasma proteins was consistent with the results from X-ray crystallography (PDB: 1E78, 1S0Q, 2BLI, and 3AT5) (Table 1), indicating that FT-IR is a suitable technique for analyzing the secondary structure of these proteins.

Table 1 Secondary structure components of selected plasma proteins determined by FT-IR spectroscopy.

Proteins	α-helix (%)		β-structure (%)		Others (%)	
	X-Ray[a]	FT-IR[b]	X-Ray	FT-IR	X-Ray	FT-IR
HSA	73.2	71.3	19.4	22.0	7.4	6.7
TRP	17.9	20.3	63.2	61.7	18.8	8.0
MB	79.4	76.5	14.7	18.7	5.9	4.8
HB	75.6	76.7	16.7	18.5	7.7	4.8

[a]Data from PDB; [b]Data from FT-IR analysis.

To analyze the structural changes in select plasma proteins absorbed on Au/AgNPs, the FT-IR secondary derivative spectra of these proteins absorbed on Au/AgNPs were recorded at different incubation times. HB and MB did not have any sulfur. However, TRP contains a cysteine and six disulfide bridges[33] and HSA contains a cysteine and 17 pairs of disulfides.[34] The structural changes in non-thio-proteins (HB and MB) absorbed on AuNPs are shown in Fig. 1. There were no changes in the secondary structural composition as a function of incubation time. The FT-IR second-derivative spectra for the MB/HB-AgNP complex showed the same results (data not shown).

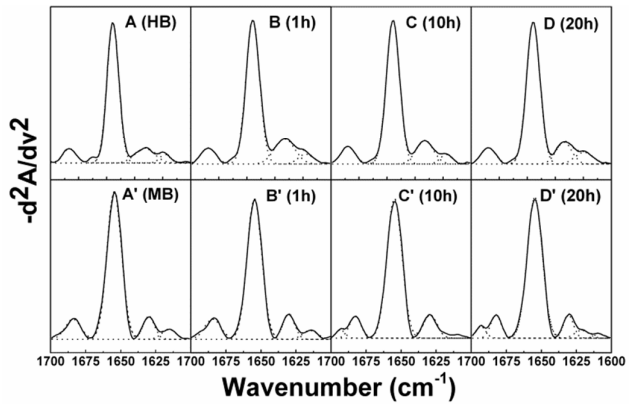

Fig. 1 Curve-fitted inverted second-derivative amide I spectra of HB (A, B, C, D) and MB (A', B', C', D') absorbed on 40 nm AuNPs at different incubation times.

The structural changes in thio-proteins (TRP and HSA) absorbed on AuNPs or AgNPs are shown in Fig. 2 and 3. Fig. 2 shows significant changes in the secondary structural composition of TRP-AuNPs as a function of incubation time. The intensities of α-helix bands (1658, 1665 cm^{-1}) decreased, whereas β-sheets (1630 and 1640 cm^{-1}) and random coil bands (1649 cm^{-1}) increased. The FT-IR second-derivative spectra for the TRP-AgNP complex showed the same results (data not shown).

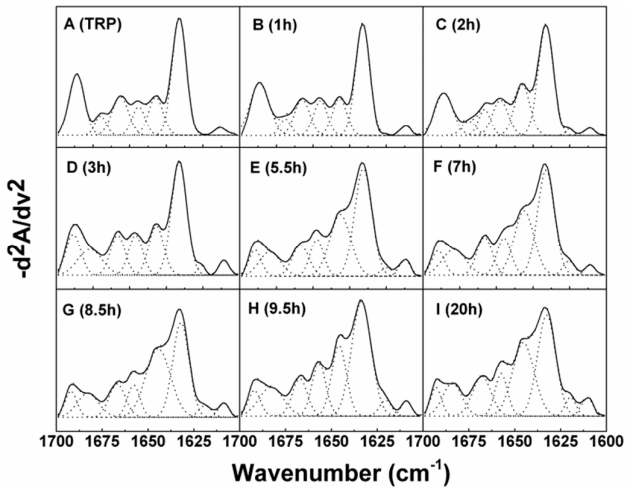

Fig. 2 Curve-fitted inverted second-derivative amide I spectrum of TRP absorbed on 40 nm AuNPs at different incubation times.

Fig.3 presents the relative amounts of different structural components of HSA absorbed on HSA-AgNPs. The intensities of α-helix bands (1658, 1665 cm^{-1}) decreased, whereas β-sheets (1630 and 1640 cm^{-1}) increased (data for HSA-AuNPs were reported previously[21]). Fig. 3 and 4 indicate that the secondary structures of HSA and TRP underwent changes over time after absorption on AuNPs or AgNPs. Comparing the results of thio- and non-thio-proteins, we conclude that the change in the secondary structure of plasma proteins absorbed on AuNPs or AgNPs is induced by sulfur-Au (or Ag) interactions.

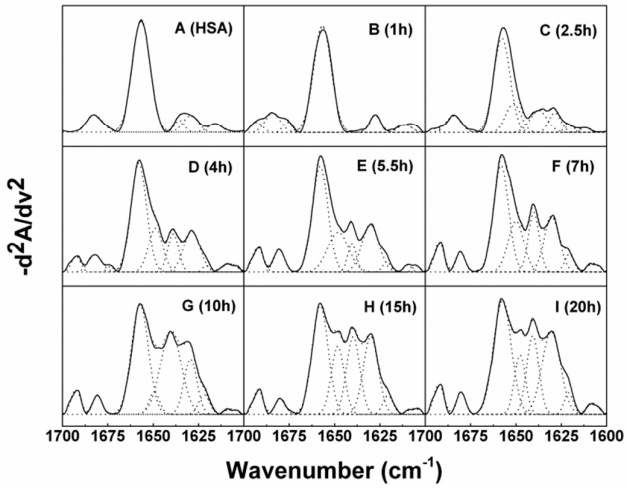

Fig. 3 Curve-fitted inverted second-derivative amide I spectrum of HSA absorbed on 40 nm AgNPs at different incubation times.

Comparing the results for AuNPs and AgNPs, we found that the incubation times to reach structurally stable TRP or HSA are different. The TRP-AuNP interaction requires approximately 10 hours, whereas TRP-AgNPs require 14 hours to reach structural stability. Similarly, the HSA-AuNP interaction requires approximately 8 hours and HSA-AgNPs 15 hours to reach structural stability. The relative intensities of α-helix interactions are shown in Fig. 4. The bond energy of Au-S and Ag-S is approximately 268.2-239.0 KJ/mol and 231.3-202.1 KJ/mol, respectively.[35] The reaction of the protein absorbed on AuNPs or AgNPs needs to break disulfide bonds and form the S-Au (or Ag) bond[20]; the higher the bond energy, the less reaction time needed. As shown in Fig. 4, the incubation time for structural changes in thio-proteins absorbed on NPs depends on the sulfur-metal bond energy; the stronger the sulfur-metal energy, the less incubation time needed.

Proteins can be absorbed on the surface of AuNPs very quickly by electrostatic force.[24] For thio-proteins, the disulfide bonds are usually located in different places, some are most likely on the surface and easily make with contact Au/Ag, whereas some are located in flexible buried regions and take time to come into contact with NPs. Yet others are located in the core region of the protein, which may take even longer to come into contact with NP. This may be the reason for a change in protein structure over incubation time with AuNPs or AgNPs. The possible mechanism for plasma proteins absorption on AuNP or AgNP can be described: For non-thio-proteins, absorption is due to the fast electrostatic force. For thio-proteins, absorption is due to a fast electrostatic force followed by slow formation of a covalent bond (S-Au or S-Ag coordination).

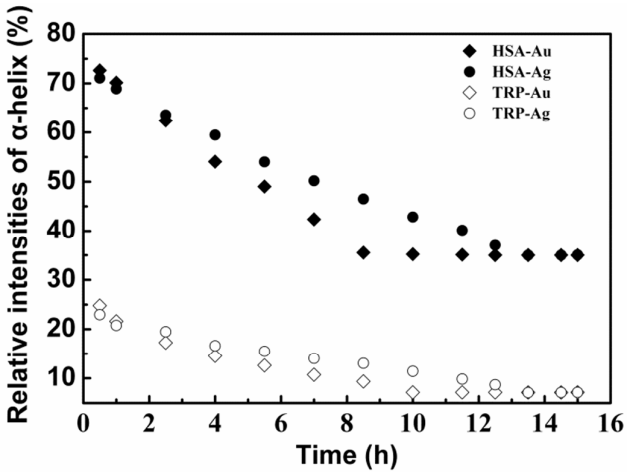

Fig.4 Effects of Au/AgNPs on the relative amount of α-helix in HSA-Au (◆), HSA-Ag (●), TRP-Au(◇), and TRP-Ag(○) over incubation time.

To explore the effect of AuNPs and AgNPs on the intrinsic structural dynamic and conformational flexibility of selected plasma proteins, we carried out H-D exchange experiments and monitored the proton exchange rate in proteins using FT-IR spectroscopy. A particular advantage of H-D exchange lies in its capacity to characterize transient conformations, which may represent a negligible, and difficult to detect, fraction of all protein molecules.[36] Fig. 5 is an overlay of the representative absorption spectra of HSA and HSA-AuNPs recorded at 1, 3, 5, 9, 10, 30, 90, 120 and 180 min of exposure to D_2O with the spectra of the protein in H_2O as a reference.

HSA in H_2O exhibited characteristic amide I and II band maxima at 1656/54 and 1546 cm^{-1}, respectively. The H-D exchange of HSA-AuNPs in D_2O led to a time-dependent isotopic shift of the amide II band from 1564 to 1454 cm^{-1}.

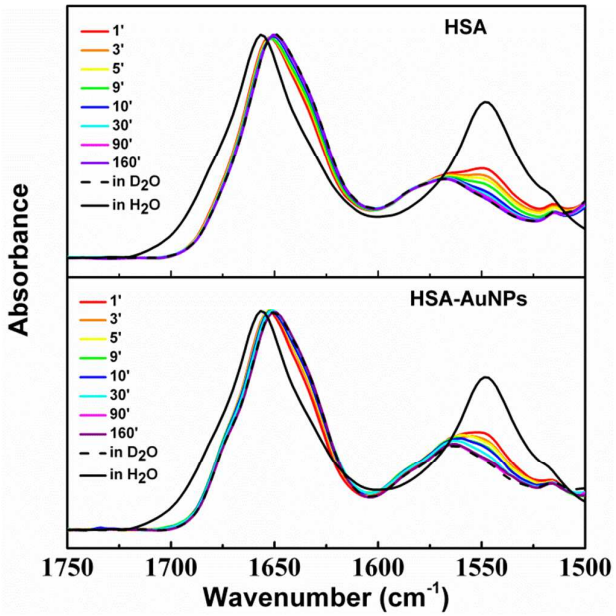

Fig. 5 H-D exchange of HSA and HSA-AuNPs determined by FT-IR spectroscopy. Spectra for the protein in H_2O are included for comparison. Data for HB, MB, and TRP are not shown.

The overall H–D exchange rates for HSA and HSA-AuNPs at different molar ratios were estimated by plotting the fraction of unexchanged amide protons, calculated from the amide II band using Eq. (1), as a function of time. The results of all H/D exchange experiments are shown in Fig. 6. Only a small fraction existed in the percentage of unexchanged amide protons from HSA at the first time point (1 min). The high level of exchange is consistent with the highly flexible and dynamic nature of HSA protein. A remarkable increase (~2.5%) was measured in the rate of unexchanged amide protons from HSA after adsorption on AuNPs at the first time point (1 min). For TRP, the fraction of unexchanged amide protons at the first time point (1 min) increased by ~1.7% after adsorption on AuNPs. For the non-thio-proteins, no significant increase was observed at the first time point (1 min) after adsorption on AuNPs. These observations suggest that the protein-NP complex with thio-proteins is less dynamic than that of free proteins. No measurable dynamic differences were found between free non-thio-protein and protein-Au/AgNP complexes. These results indicate that covalent bonds have a greater impact on protein structure and function than that of electrostatic force.

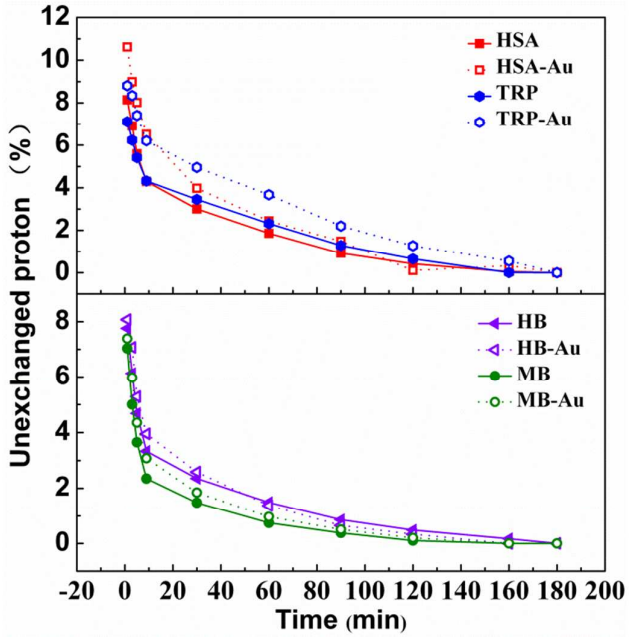

Fig. 6 The H-D exchange rate of selected plasma proteins in the absence and presence of AuNPs. The fraction of unexchanged amide protons as a function of time was calculated using Eq.(1). The lines represent the best fit of the data using a two-exponent function (Eq.(2)).

Experimental

Materials

HSA expressed in rice, MB from equine heart, TRP from bovine pancreas were purchased from Sigma Aldrich (USA) and used without further purification. We cloned HB gene from bovine pancreas to get HBαC92A mutant, and purified as published procedures.[37] Deuterium oxide (99.9 atom % D) was purchased from J&K Chemical Ltd. AuNPs and AgNPs (40nm diameter) were procured from Sigma. The stock solutions of proteins with Au/AgNPs were prepared in 0.01 M phosphate buffer solution (PBS; pH 7.0)(in AuNPs) and sodium citrate(pH 7.0) (in AgNPs).

Preparation of Protein-NP complex

Protein coronas (protein-AuNPs or AgNPs) were obtained by incubating protein (200µl, 20 mg/ml) with NPs (1000µl, ~7.0×10^{10} particles/ml) for 10 min at room temperature. After incubation, the samples were centrifuged for 1 min at 10,000 rpm and the buffer and unbound proteins removed. 50 µl of 0.01 M phosphate buffer solution (pH 7.0, for AuNPs) or 0.01 M sodium citrate solution (pH 7.0, for AgNPs) was added to re-suspend the protein-Au/AgNP complexes. This procedure was repeated three times to wash the sample and remove free proteins not bound to the Au/AgNPs. Both DLS (dynamic light scattering) and TEM (transmission electron microscope)

images revealed that proteins were absorbed on the surface of NPs and well-dispersed in solution (data not shown). The secondary structures of proteins absorbed on Au/AgNPs were based on an analysis of the amide I band in FT-IR spectroscopy.

FTIR spectroscopy

FT-IR spectra were recorded with an ABB Bomem (Quebec, Canada) MB-3000 Fourier transform infrared spectrometer equipped with a deuterated triglycine sulfate detector and purged constantly with dry air. Frozen protein samples were thawed at room temperature and loaded into a liquid IR cell with CaF_2 windows and 7.5-μm spacer. For each spectrum, a 128-scan interferogram was collected in single-beam mode with 4cm^{-1} resolution at room temperature. The reference spectrum was recorded under identical conditions with only the corresponding buffer in the cell. The protein spectra were processed using a previously established protocol.[38,39] A straight baseline between 2000 and 1750 cm^{-1} was used as the standard for judging the success of water subtraction. Second-derivative spectra were obtained using a seven-point baseline-corrected Savitzky–Golay derivative function, and the amide I band was area-normalized as described previously.[38] The secondary structure content of the protein was calculated by curve-fitting analysis of the inverted second-derivative amide I band from 1600 to 1700 cm^{-1}.[40] The amide I band was ascribed to the C=O stretching vibration of the peptide bond.[41] The fraction of amino acid residues comprising each secondary structural element was proportional to the relative percent area of the associated C=O vibrational bands.[39,42]

Hydrogen-deuterium exchange

Protein-NP complexes were obtained by incubating protein (200 μl, 20 mg/ml) with NPs (1000 μl, ~7.0×10^{10} particles/ml) for 10 min at room temperature. The samples were then lyophilized using a LNG-T98A Lyophilizer. The H–D exchange experiments were performed by reconstituting lyophilized protein samples with 50 μl of D_2O and injecting the sample immediately into an IR cell with CaF_2 windows and 50-μm spacer. The spectral measurements were started 1 min (i.e., lag time = 1 min) after the addition of D_2O using the kinetic scanning mode. The spectra were recorded at 1–11, 15, 20, 30, 40, 50, 60, 90, 120 and 180 min. An 8-scan interferogram was collected at each time interval between 1 and 10 min, whereas a 64- or 128-scan interferogram was recorded at each time interval between 11 and 90 min and later time points. For comparison, the amide I band maximum for protein in H_2O was normalized to the amide I band maximum for protein in D_2O at 1 min.

The H–D exchange process was monitored by following the apparent changes in intensity at the amide II band maxima around 1548 cm^{-1}, which was attributed to an out-of-phase combination of N–H in-plane bending and CN stretching vibrations in the peptide bonds. The absorption bands arising from H_2O, HOD, or D_2O do not interfere with the amide II band.[41] As the protein amide N–H bonds in H_2O change to N–D bonds in D_2O, the N–H bending vibrational band at 1550 cm^{-1} decreases and the magnitude of the N–D bending vibrational band at 1450 cm^{-1} increases. The fraction of unexchanged amide proton, F, was calculated at various time intervals using Eq. (1).[32]

$$F=(A_{II}-A_{II\infty})/A_I\omega \quad (1)$$

In Eq. (1), A_I and A_{II} are the absorbance maxima of the amide I and II bands, respectively; $A_{II\infty}$ is the amide II absorbance maximum of the fully deuterated protein; and ω is the ratio of A_{II}/A_I, with A_{II} and A_I being the absorbance maxima for the amide II and amide I bands of protein in H_2O, respectively. The exchange kinetic parameters were fitted using Eq. (2).[43]

$$F=A_1e^{-k1t}+A_2e^{-k2t}+C \quad (2)$$

In Eq. (2), F is the amide proton fraction at time t; k_1 and k_2 are the intermediate and slow exchange rates, respectively; and A_1, A_2, and C are constants.[3]

Conclusions

In summary, the absorption of plasma proteins on NPs occurs mainly due to a fast electrostatic force and slow formation of covalent bonds. Secondary structural changes do not occur in non-thio-proteins (HB and MB). However, the secondary structures of thio-proteins (HSA and TRP) changed over time due to absorption on AuNP or AgNP. A longer interaction time is needed for AgNPs to achieve a stable thio-protein structure compared to AuNPs, indicating that the interaction time for structural changes depends on the sulfur-metal bond energy; the stronger the sulfur-metal energy, the less interaction time needed. Thio-protein-NP complexes were also less dynamic than that of free proteins. On the other hand, no measurable dynamic differences were found between free non-thio-proteins and protein-AuNP (or AgNP) complexes. These results revealed that the impact of covalent bonds on protein structure is much greater than that of electrostatic forces. This result may extend to bio-applications with other nano materials.

Acknowledgements

The work was supported by the National Natural Science Foundation of China (No.21275032, 31470786, and 81372355) and the Special Major Science and Technology Foundation of China (No. 2012ZX10002-017).

Notes and references

1 J. Klein, *Proceedings of the National Academy of Sciences*, 2007, **104**, 2029-2030.
2 T. Cedervall, I. Lynch, S. Lindman, T. Berggard, E. Thulin, H. Nilsson, K. A. Dawson and S. Linse, *Proceedings of the National Academy of Sciences*, 2007, **104**, 2050-2055.

3 L. Wang, J. Li, J. Pan, X. Jiang, Y. Ji, Y. Li, Y. Qu, Y. Zhao, X. Wu and C. Chen, *Journal of the American Chemical Society*, 2013, **135**, 17359-17368.
4 M. Lundqvist, J. Stigler, G. Elia, I. Lynch, T. Cedervall and K. A. Dawson, *Proceedings of the National Academy of Sciences* 2008, **105**, 14265-14270.
5 E. Casals, T. Pfaller, A. Duschl, G. J. Oostingh and V.Puntes, *ACS Nano*, 2010, **4**, 3623–3632.
6 T. Cedervall, I. Lynch, M. Foy, T. Berggad, S. Donnelly, G. Cagney and S. Linse, *Angew Chem Int Ed*, 2007, **46**, 5754–5756.
7 R. Landsiedel, et al, *Adv Mater*, 2010, **22**, 2601–2627.
8 M. Lundqvist, I. Sethson and B. H. Jonsson, *Langmuir*, 2004, **20**, 10639–10647.
9 M. Lundqvist, I. Sethson and B. H. Jonsson, *Biochemistry*, 2005, **44**, 10093–10099.
10 S. S. Karajanagi, A. A. Vertegel, R. S. Kane and J. S. Dordick, *Langmuir*, 2004, **20**, 11594–11599.
11 M. P. Monopoli, D. Walczyk, A. Campbell, G. Elia, I. Lyncha and F. BaldelliBombelli, *J Am ChemSoc*, 2011, **133**, 2525–2534.
12 J. Mariam, S. Sivakami, D. Kothari and P. Dongre, *The protein journal,* 2014, **33**, 258-266.
13 S. R. Saptarshi, A. Duschl and A. L. Lopata, *J Nanobiotechnol*, 2013, **11**.
14 B. Wang, C. Guo, Z. Lou and B. Xu, *Chemical Communications*, 2015.
15 M. V. Canamares, J. V. Garcia-Ramos, J. D. Gomez-Varga, C. Domingo and S. Sanchez-Cortes, *Langmuir*, 2005, **21**, 9303-9307.
16 A. G. Tkachenko, H. Xie, D. Coleman, W. Glomm, J. Ryan, M. F. Anderson, S. Franzen and D. L. Feldheim,*Journal of the American Chemical Society*, 2003, **125**, 4700-4701.
17 L. M. Demers, C. A. Mirkin, R. C. Mucic, R. A. Reynolds, R. L. Letsinger, R. Elghanian and G. Viswanadham, *Analytical Chemistry*, 2000, **72**, 5535-5541.
18 T. A. Taton, C. A. Mirkin and R. L. Letsinger, *Science*, 2000, **289**, 1757-1760.
19 Z. J. Deng, M. T. Liang, I. Toth, M. Monteiro and R. F. Minchin, *Nanotoxicology*, 2013, **7**, 314-322.
20 D. Zhang, O. Neumann, H. Wang, V. M. Yuwono, A. Barhoumi, M. Perham, J. D. Hartgerink, P. Wittung-Stafshede and N. J. Halas, *Nano letters*, 2009, **9**, 666-671.
21 C. P. Fu, H. Y. Yang, M. M. Wang, H. M. Xiong and S. N. Yu，*Chemical Communications*, 2015, **51**, 3634-3636.
22 D. Wu, J. Yan, J. Wang, Q. Wang and H. Li, *Food chemistry*, 2015, **170**, 423-429.
23 M. Voicescu, S. Ionescu and D. G. Angelescu, *Journal of Nanoparticle Research*, 2012, **14**.
24 M. Lundqvist, *Nature nanotechnology*, 2013, **8**, 701-702.
25 E. Sanfins, J. Dairou, F. Rodrigues-Lima and J.-M. Dupret, *Journal of Physics: Conference Series*, 2011, **304**, 1742-6596.
26 X. R. Xia, N. A. Monteiro-Riviere and J. E. Riviere, *Nature nanotechnology,* 2010, **5**, 671-675.
27 J. W. Park and J. S. Shumaker-Parry, *Journal of the American Chemical Society,* 2014, **136**, 1907-1921.
28 C. Mathe, S. Devineau, J. C. Aude, G. Lagniel, S. Chedin, V. Legros, M. H. Mathon, J. P. Renault, S. Pin, Y. Boulard and J. Labarre, *Plos One,* 2013, **8**.
29 J. Visser, *Powder Technol*, 1989, **58**, 1–10.
30 S. Chakraborti, P. Joshi, D. Chakravarty, V. Shanker, Z. A. Ansari, S. P. Singh and P. Chakrabarti, *Langmuir* 2012, **28**, 11142.
31 H. Yang, S. Yang, J. Kong, A. Dong and S. Yu, *Nature Protocols*, 2015, **10**, 382-396.
32 J. Kong and S. Yu, *Acta Biochimica et Biophysica Sinica,* 2007, **39**, 549-559.
33 E. Blankenship, K. Vukoti, M. Miyagi and D. T. Lodowski, *Acta Crystallographica Section D-Biological Crystallography*, 2014.
34 M. A. Dobrovolskaia, A. K. Patri, J. W. Zheng, J. D. Clogston, N. Ayub, P. Aggarwal, B. W. Neun, J. B. Hall and S. E. McNeil, *Nanomedicine-Nanotechnology Biology and Medicine*, 2009, **5**, 106-117.
35 Y. R. Luo, *Comprehensive Handbook of Chemical Bond Energies,* CRC Press, Boca Raton, 2007.
36 W. Dzwolak, A. Loksztejn and V. *Smirnovas, Biochemistry*, 2006, **45**, 8143-8151.
37 C. T. Andrade, L. A. M. Barros, M. C. P. Lima and E. G. Azero, *International Journal of Biological Macromolecules,* 2004, **34**, 233-240.
38 A. C. Dong and W. S. Caughey, *Hemoglobins*, *Pt C,* 1994, **232**, 139-175.
39 A. C. Dong, P. Huang and W. S. Caughey, *Biochemistry*, 1990, **29**, 3303-3308.
40 A. C. Dong, J. M. Malecki, L. Lee, J. F. Carpenter and J. C. Lee, *Biochemistry*, 2002, **41**, 6660-6667.
41 C. Jung, Journal of Molecular Recognition, 2000, **13**, 325-351.
42 D. M. Byler and H. Susi, *Biopolymers*, 1986, **25**, 469-487.
43 A. D.Barksdale and A. Rosenberg, *Methods of Biochemical Analysis*, 1982, **28**, 1-113.